

Dynamic simulation of the Wilberforce pendulum using constrained spatial nonlinear beam finite elements

Jonas Harsch^{1,*}, Giuseppe Capobianco¹, and Simon R. Eugster¹

¹ Institute for Nonlinear Mechanics, University of Stuttgart, Stuttgart, Germany

More than 100 years ago, Lionel Robert Wilberforce did investigations *On the Vibrations of a Loaded Spiral Spring* [1]. The spring was clamped at its upper side and on the other side, perpendicular to the spring axis, a steel cylinder was attached. Four screws with adjustable nuts were symmetrically attached around the cylinder in order to change its moment of inertia (Fig. 1). In this paper the Wilberforce pendulum is modeled by a rigid body attached to a constrained spatial nonlinear Timoshenko beam, discretized with B-spline shape functions. As shown by a numerical experiment, the presented model is capable of reproducing the characteristic pendulum motion.

© 2021 The Authors. *Proceedings in Applied Mathematics & Mechanics* published by Wiley-VCH GmbH.

The pendulum's spring is made of spring steel EN 10270-1 with density $\rho_0 = 7850 \text{ kg/m}^3$, Young's modulus $E = 206 \cdot 10^9 \text{ N/m}^2$ and shear modulus $G = 81.5 \cdot 10^9 \text{ N/m}^2$. Has the undeformed shape of a perfect helix with $n = 20$ coils, coil radius $R = 16 \text{ mm}$, wire diameter $d = 1 \text{ mm}$ and unloaded pitch $c = 1 \text{ mm}$. It is discretized using 128 cubic uniformly distributed B-spline finite elements of the Timoshenko beam model presented in [2].

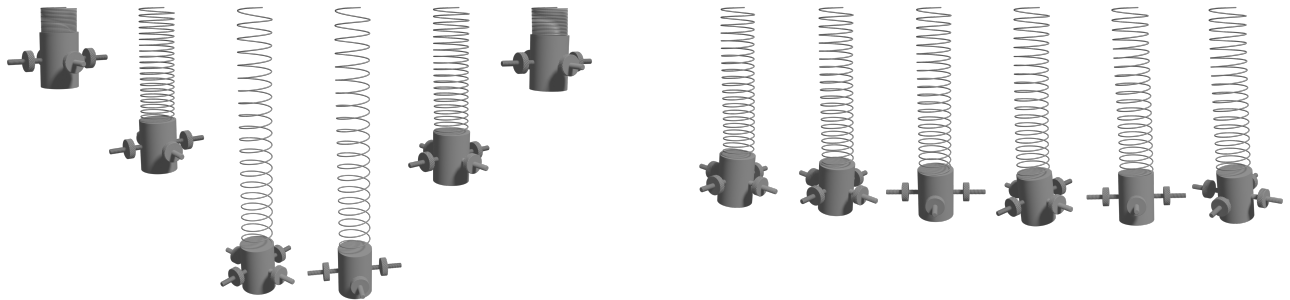


Fig. 1: Configurations of the Wilberforce pendulum: (left) pure vertical oscillations, (right) pure torsional oscillation of the pendulum bob.

The motion of the beam's centerline is given by the mapping $\mathbf{r} : I \times \mathbb{R} \rightarrow \mathbb{E}^3, (\xi, t) \mapsto \mathbf{r}(\xi, t)$, where, for each instant of time $t \in \mathbb{R}$, the closed unit interval $I = [0, 1] \subset \mathbb{R}$ parametrizes the set of beam points in the three dimensional Euclidean space \mathbb{E}^3 , which comes with a right-handed orthonormal basis $(\mathbf{e}_1, \mathbf{e}_2, \mathbf{e}_3)$. It is further augmented by the motion of positively oriented orthonormal director triads $\mathbf{d}_i : I \times \mathbb{R} \rightarrow \mathbb{E}^3, i = 1, 2, 3$ in order to capture the beam's cross-sectional orientations. The directors $\mathbf{d}_\alpha(\xi, t), \alpha = 2, 3$ span the plane and rigid cross section. The placement of the reference centerline is given by

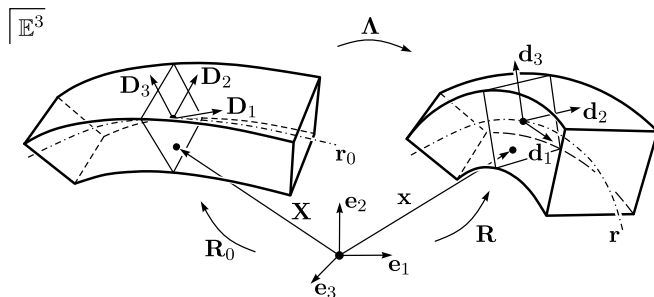


Fig. 2: Kinematics of the precurved spatial Timoshenko beam.

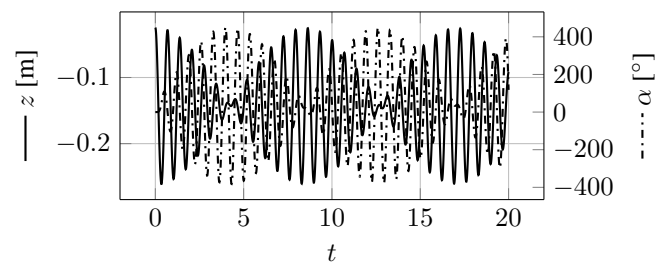


Fig. 3: Deflection and first Cardan angle of the pendulum bob.

$\mathbf{r}_0 : I \rightarrow \mathbb{E}^3$ and the corresponding orthonormal director triads are $\mathbf{D}_i : I \rightarrow \mathbb{E}^3$. While \mathbf{D}_1 is identified with the unit tangent to the reference centerline \mathbf{r}_0 , i.e., $\mathbf{D}_1 = \mathbf{r}'_0 / \|\mathbf{r}'_0\|$ with $\mathbf{r}'_0 := \frac{\partial \mathbf{r}_0}{\partial \xi}$, the vectors \mathbf{D}_2 and \mathbf{D}_3 are identified with the geometric principal axes of the cross sections, see Figure 2. Since a helix is a transcendental curve that can be represented exactly by

$$\mathbf{r}_0^*(\xi) = R \cos \phi(\xi) \mathbf{e}_1 + R \sin \phi(\xi) \mathbf{e}_2 + c \xi \mathbf{e}_3, \quad \phi(\xi) = 2\pi n \xi, \quad (1)$$

there is no exact representation for it by means of rational functions, e.g., B-splines. Thus, in order to obtain a helicoidal beam reference configuration, a fitting procedure is required. This was done by minimizing the quadratic error $e_k = \sum_{i=1}^k \|\mathbf{r}_0(\xi_i) -$

* Corresponding author: harsch@inm.uni-stuttgart.de



This is an open access article under the terms of the Creative Commons Attribution-NonCommercial-NoDerivs License, which permits use and distribution in any medium, provided the original work is properly cited, the use is non-commercial and no modifications or adaptations are made.

$\mathbf{r}_0^*(\xi_i)\|^2$ of the beam's reference centerline [3]. For obtaining the beam's orientations the very same procedure was applied by replacing the difference of the beam's reference centerline with the difference of each director \mathbf{d}_i and its corresponding vector of the helix space curve's Serret-Frenet frame.

Next, by introducing the arc length coordinate $s = \int_0^\xi J(\xi) d\bar{\xi}$ of the reference centerline at ξ , together with $J(\xi) := \|\partial \mathbf{r}_0(\xi)/\partial \xi\|$, the respective differential measures ds and $d\xi$ of the arc length and the parameter domain can be related by $ds = J(\xi)d\xi$. Let f be an arbitrary mapping $f: I \times \mathbb{R} \rightarrow \mathbb{E}^3$, $(\xi, t) \mapsto f(\xi, t)$, its derivative with respect to the arc length of the reference centerline is defined as $\frac{\partial f}{\partial s}(\xi, t) := \frac{\partial f}{\partial \xi}(\xi, t)/J(\xi)$.

Further, by defining an appropriate strain energy density $W(\Gamma_i, K_i; \xi)$, see [2], and application of Einstein summation convention on repeated indices, the beam's material resistance is modeled by the internal virtual work

$$\delta W^{\text{int}} = - \int_I \left\{ \delta \mathbf{r}' \cdot n_i \mathbf{d}_i + \delta \mathbf{d}_i \cdot (n_i \mathbf{r}' + \varepsilon_{kji} \frac{m_k}{2} \mathbf{d}'_j) + \delta \mathbf{d}'_j \cdot \varepsilon_{ijk} \frac{m_i}{2} \mathbf{d}_k \right\} d\xi, \quad (2)$$

where the contact forces $n_i(\xi, t) = \frac{\partial W}{\partial \Gamma_i}(\Gamma_i(\xi, t), K_i(\xi, t); \xi)$ and contact couples $m_i(\xi, t) = \frac{\partial W}{\partial K_i}(\Gamma_i(\xi, t), K_i(\xi, t); \xi)$ depend on the objective strain measures $\Gamma_i(\xi, t) = \mathbf{r}'(\xi, t) \cdot \mathbf{d}_i(\xi, t)/J(\xi)$, $K_i(\xi, t) = \frac{1}{2} \varepsilon_{ijk} \mathbf{d}_k(\xi, t) \cdot \mathbf{d}'_j(\xi, t)/J(\xi)$ and possibly on the material point ξ itself.

Gravitational effects are incorporated by the external virtual work $\delta W^{\text{ext}} = \int_I \delta \mathbf{r} \cdot \bar{\mathbf{n}} J d\xi$, where the vector of gravitational forces $\bar{\mathbf{n}} = -\rho_0 A g \mathbf{e}_2$, the beam's cross sectional area $A = \pi(d/2)^2$ and the gravitational acceleration g were introduced.

In order to formulate the virtual work contributions of inertia effects, the beam is assumed to be a constrained three-dimensional continuous body [4,5] whose points in the current configuration are restricted to $\mathbf{x}(\xi, \theta_\alpha, t) = \mathbf{r}(\xi, t) + \theta_\alpha \mathbf{d}_\alpha(\xi, t)$. Here $(\xi, \theta_2, \theta_3) \in \mathcal{B} \subset \mathbb{R}^3$ are chosen such that they address the whole beam volume in its reference configuration. Thus, inserting this restricted kinematics into the commonly used virtual work of the inertia forces of a three-dimensional continuous body yields

$$\delta W^{\text{dyn}} = - \int_{\mathcal{B}} \delta \mathbf{x} \cdot \ddot{\mathbf{x}} dm = - \int_0^1 \left\{ \delta \mathbf{r} \cdot (A_{\rho_0} \ddot{\mathbf{r}} + B_{\rho_0}^\alpha \ddot{\mathbf{d}}_\alpha) + \delta \mathbf{d}_\alpha \cdot (B_{\rho_0}^\alpha \ddot{\mathbf{r}} + C_{\rho_0}^{\alpha\beta} \ddot{\mathbf{d}}_\beta) \right\} J d\xi, \quad (3)$$

where the constant integrated quantities $A_{\rho_0} = \int_A \rho_0 dA$, $B_{\rho_0}^\alpha = \int_A \rho_0 \theta_\alpha dA$ and $C_{\rho_0}^{\alpha\beta} = \int_A \rho_0 \theta_\alpha \theta_\beta dA$ have been introduced.

For the used director beam formulation one must enforce the requirement of $\mathbf{d}_i \otimes \mathbf{e}_i: I \times \mathbb{R} \rightarrow \text{Orth}^+$ to be a proper rotation, i.e., the directors must remain orthonormal throughout the motion. This leads to six independent constraint equations $g_{ij}(\xi, t) = \mathbf{d}_i(\xi, t) \cdot \mathbf{d}_j(\xi, t) - \delta_{ij} = 0$, with $1 \leq i \leq j \leq 3$. These constraints are incorporated into the principle of virtual work by the contribution

$$\delta W^c = \int_I \left\{ \delta \lambda_{ij} (\mathbf{d}_i \cdot \mathbf{d}_j - \delta_{ij}) + (\delta \mathbf{d}_i \cdot \mathbf{d}_j + \delta \mathbf{d}_j \cdot \mathbf{d}_i) \lambda_{ij} \right\} d\xi. \quad (4)$$

Finally, the pendulum bob is modeled as a spatial rigid body of mass $m = 0.469$ kg and moment of inertia in the body fixed frame given by a diagonal matrix with entries $\Theta_{00} = \Theta_{11} = 0.0001468$ kg m² and $\Theta_{22} = 0.0001247$ kg m². It is parametrized using the Cardan angles z - x' - y'' , starting from $\mathbf{e}_x = \mathbf{e}_1$, $\mathbf{e}_y = \mathbf{e}_2$ and $\mathbf{e}_z = \mathbf{e}_3$.

When the cylinder is displaced vertically subjected to gravitational forces, it starts oscillating up and down (Fig. 1). Due to the coupling of bending and torsion of the deformed spring an additional torsional oscillation of the cylinder is induced (Fig. 1). When the cylinder's moment of inertia is properly adjusted, the vertical and torsional oscillation possess an almost perfect phase shift of $\pi/2$, i.e., the maximal amplitude of the vertical oscillation coincides with a zero torsional amplitude and vice versa. Using the generalized- α scheme [6] for constrained mechanical systems of index 3, an integration time $T = 20$ s, a time step $\Delta t = 5 \cdot 10^{-4}$ s and the spectral radius at infinity $\rho_\infty = 0.5$, the eccentricity of the adjustable nuts was optimized leading to the given values for the moment of inertia in order to achieve an almost perfect phase shift shown in Fig. 3.

Acknowledgements This research has been funded by the Deutsche Forschungsgemeinschaft (DFG, German Research Foundation) under Grant No. 405032572 as part of the priority program 2100 Soft Material Robotic Systems. Open access funding enabled and organized by Projekt DEAL.

References

- [1] L. R. Wilberforce, The London, Edinburgh, and Dublin Philosophical Magazine and Journal of Science **38**(233), 386–392 (1894).
- [2] J. Harsch, G. Capobianco, and S. R. Eugster, Mathematics and Mechanics of Solids(0), 1–26 (2021).
- [3] L. A. Pieggl and W. Tiller, The NURBS Book, 2. edition (Springer, Berlin; Heidelberg, 1997).
- [4] S. R. Eugster, On the Foundations of Continuum Mechanics and its Application to Beam Theories, PhD thesis, ETH Zurich, 2014.
- [5] S. R. Eugster and J. Harsch, A variational formulation of classical nonlinear beam theories, in: Developments and Novel Approaches in Nonlinear Solid Body Mechanics, edited by B. E. Abali and I. Giorgio (Springer, 2020).
- [6] M. Arnold and O. Brülls, Multibody System Dynamics **18**(2), 185–202 (2007).